Chinese Journal of Physics 56 (2018) 1743–1755

Contents lists available at ScienceDirect

Chinese Journal of Physics

journal homepage: www.elsevier.com/locate/cjph

Structural and electronic properties of $Sb_nAl^{(0,\pm 1)}$ (n = 1–10) clusters using density-functional theory

Zhang Y.X.[a], Shi S.P.[a,*], Liu Y.L.[b], Yan M.[a], Zhao X.F.[a], Jiang G.[c]

[a] Department of Applied Phys., College of Geophysics, Chengdu University of Technology, Chengdu 610059, China
[b] College of Electrical and Information Engineering, Southwest University for Nationalities, Chengdu 610041, China
[c] Institute of Atomic and Molecular Phys., Sichuan University, Chengdu 610065, China

ARTICLE INFO

Keywords:
$Sb_nAl^{(0,\pm 1)}$ clusters
DFT
Stability
Electronic property

ABSTRACT

We used the density functional theory (DFT) with the unrestricted B3LYP exchange-correlation potential and LanL2DZ basis sets to optimize the geometries of Sb_nAl and $Sb_nAl^{\pm 1}$ (n = 1–10) clusters. We mainly utilized Gaussian 03 W software to calculate the data. In order to find the most stable structure of each isomer, we calculated the total energy, the spin multiplicity (S), point group symmetry (PG), the electronic state (State), and the average bond lengths of Sb-Al bond and Sb-Sb bond (R_1 and R_2). Through the calculations and analysis of these data, we found the ground state structure of each group isomer. By discussing the average binding energy (E_b), fragmentation energy (E_f), and the second-order energy difference (Δ_2E), the stabilities of the $Sb_nAl^{(0,\pm 1)}$ clusters were studied. The results of the electron transfer show that the Sb_4Al and Sb_8Al clusters are different with the other neutral clusters. In order to study the electric properties of $Sb_nAl^{(0,\pm 1)}$ clusters, the energy gap (E_g) between the highest occupied molecular orbital (HOMO) and the lowest unoccupied molecular orbital (LUMO), AEA, VDE, AIP, and VIP were calculated. Besides, the magnetic moment of the positive and negative clusters have the same effects when n = 2–9.

1. Introduction

Over that last few decades, interest in clusters arise, in part, because they constitute a new type of material that may have properties, which are distinct from those of individual atoms and molecules or bulk matters, in terms of electronic structures, geometries, magnetisms and optical properties [1–4]. Specially, there are continuous interests in metal clusters due to their great potential applications in many fields, such as catalysis, optics, and nanoelectronics [5–11]. At present, due to the special electronic structure of the p-region elements, the application of materials constructed from p-region elements become important and crosses a wide range of areas [12]. In particular, due to the especial electronic structure of the p-region element, these elements and its oxide are widely used in photolytic water [13]. Therefore, among the many clusters, d^{10} configuration clusters (Ga, Ge, In, Sb and Sn) have been studied by many scientists due to their extensive application in catalytic materials, especially in photocatalytic water.

Sb element is one of the members of d^{10} configurations, Doping and pure antimony clusters have been studied by many researchers [14–23]. For example, Polak, with his partner, had studied the affinity of some antimony clusters [20]. They found that the Sb_2^- photoelectron spectrum displayed rich vibrational and electronic structure. Hagelberg and his team had demonstrated by Hartree-Fock method that some antimony clusters had the lowest energy in what structure [22]. Zhou *et al* had studied the structural and electronic properties of Sb_n (n = 2–10) clusters [23]. They used the density function calculation in generalized gradient

* Corresponding author.
E-mail address: shishunping13@cdut.cn (S.P. Shi).

https://doi.org/10.1016/j.cjph.2018.05.003
Received 10 February 2018; Received in revised form 8 April 2018; Accepted 4 May 2018
Available online 12 May 2018

approximation to study the structures and electronic properties of antimony clusters. And they discussed the size dependence of binding energies, the gaps between lowest-unoccupied and highest-occupied molecular orbitals, and the second-order difference of total energies.

Generally, the doping atom largely influences the electronic properties of the host clusters. For instance, when the Ti atom is doped to Ga_n clusters, the average binding energies exhibit a sequence as $Ga_nTi^- > Ga_nTi^+ > Ga_nTi > Ga_n^{+1}$, and the HOMO–LUMO gaps of Ga_nTi clusters are distinctly higher than those of Ga_n^{+1} clusters [24]. Obviously, the aluminum atom doping to other pure clusters have also a great impact to other pure clusters on property [25–29]. For instance, for doped zirconium clusters and pure zirconium clusters, as for the magnetism, the doping of Al atoms causes the spin-on moment of the host zirconium cluster to decrease [25]. Moreover, with respect to the detection of CO molecules at different levels with $Zn_{12}O_{12}$ clusters and their aluminum-doped forms, replacing a Zn atom with an Al atom slightly increases its reactivity and strongly increases its sensitivity to CO molecules [28]. As a result of the difference of electronegativity, Zhao *et al* found that about 0.5 electron transfers from the 3p orbital of Al to the 6 s orbital of Au atom through the study of the natural bond orbital analysis of Au_nAl clusters at their lowest-energy geometries [29]

Based on the study on hydrogen production from aluminum group cluster and water molecule, Ziebarth et al. studied [30] the interaction of Ga, In and Sn doped aluminum clusters and water molecules. They found that the speed and the amount of hydrogen production were significantly increased in the Al-Sn cluster, and they thought that the phenomenon was mainly due to the incorporation of the p-region metal with the d^{10} configuration in the aluminum cluster. The basic idea of this method that a cluster can therefore be assigned as a superatom analog of a specific group of the periodic table on the basis of the difference between its valence electron count and the number of electrons required to fill the nearest superatomic shell. One intriguing class of clusters, termed "superatomic", has been shown to mimic the properties of elements [31]. To our knowledge, there is no theoretical study for Al-doped Sb clusters so far. In this present paper, the structural, electronic and magnetic properties are investigated within DFT framework for small $Sb_nAl^{(0,\pm 1)}$ (n = 1–10) clusters.

2. Computation details

In this article, the density functional theory (DFT) with the unrestricted B3LYP exchange-correlation potential [32,33] and LanL2DZ basis sets [34] were used to optimize the geometries of Sb_nAl(n = 1–10) and $Sb_nAl^{\pm 1}$ (n = 1–10) clusters with different spin configurations. And the standard LanL2DZ basis sets provided an effective way to reduce difficulties in calculations of two-electron integrals caused by heavy TM atom were employed. In order to test the reliability of our calculations by the standard LanL2DZ basis sets, we compared our results with experimental results and other theory values for the bond length (R_e), vibrational frequencies (ω_e) and ionization potentials (IPs) of the Sb_2 dimer and Al_2 dimer, collected in Table 1. Results were calculated for B3LYP, B3P86, B3PW91 methods and LanL2DZ, SDD basis sets, respectively. For Sb_2, the B3P86/SDD and B3PW91/SDD results for the bond length (R_e = 2.522 Å for B3P86/SDD, R_e = 2.524 Å for B3PW91/SDD) and the vibrational frequencies (ω_e = 278.4 cm^{-1} for

Table 1
The computed spin multiplicities, bond lengths (R_e), vibrational frequencies (ω_e), and ionization potentials (IP) of dimers (Sb_2, and Al_2) and available experimental and previous theoretical data.

Molecule	Method		Spin	R_e (Å)	ω_e (cm^{-1})	IP(eV)
Sb_2	B3LYP	LanL2DZ	1	2.552	263.3	9.26
		SDD	1	2.529	273.6	8.78
	B3PW91	LanL2DZ	1	2.547	267.4	9.35
		SDD	1	2.524	277.9	8.90
	B3P86	LanL2DZ	1	2.545	268.0	9.89
		SDD	1	2.522	278.4	9.43
	Theory		1[a]	2.55[b]	276[b]	8.78[a]
	Experiment		1[c]	2.342[c]	270.0[c]	9.28[c]
Al_2	B3LYP	LanL2DZ	3	2.855	235.1	5.87
		SDD	3	2.590	280.9	6.16
	B3PW91	LanL2DZ	3	2.834	246.4	6.04
		SDD	3	2.569	297.8	6.41
	B3P86	LanL2DZ	3	2.839	245.9	6.54
		SDD	3	2.561	300.0	6.91
	Theory		3[i]	2.7[i]	241.2[i]	6.12[d]
	Experiment		3[k]	2.7[k]	284.2[k]	5.98[e]

[a] Ref [35]
[b] Ref [23]
[c] Ref [16]
[i] Ref. [36]
[d] Ref. [37]
[k] Ref. [38]
[e] Ref. [39].

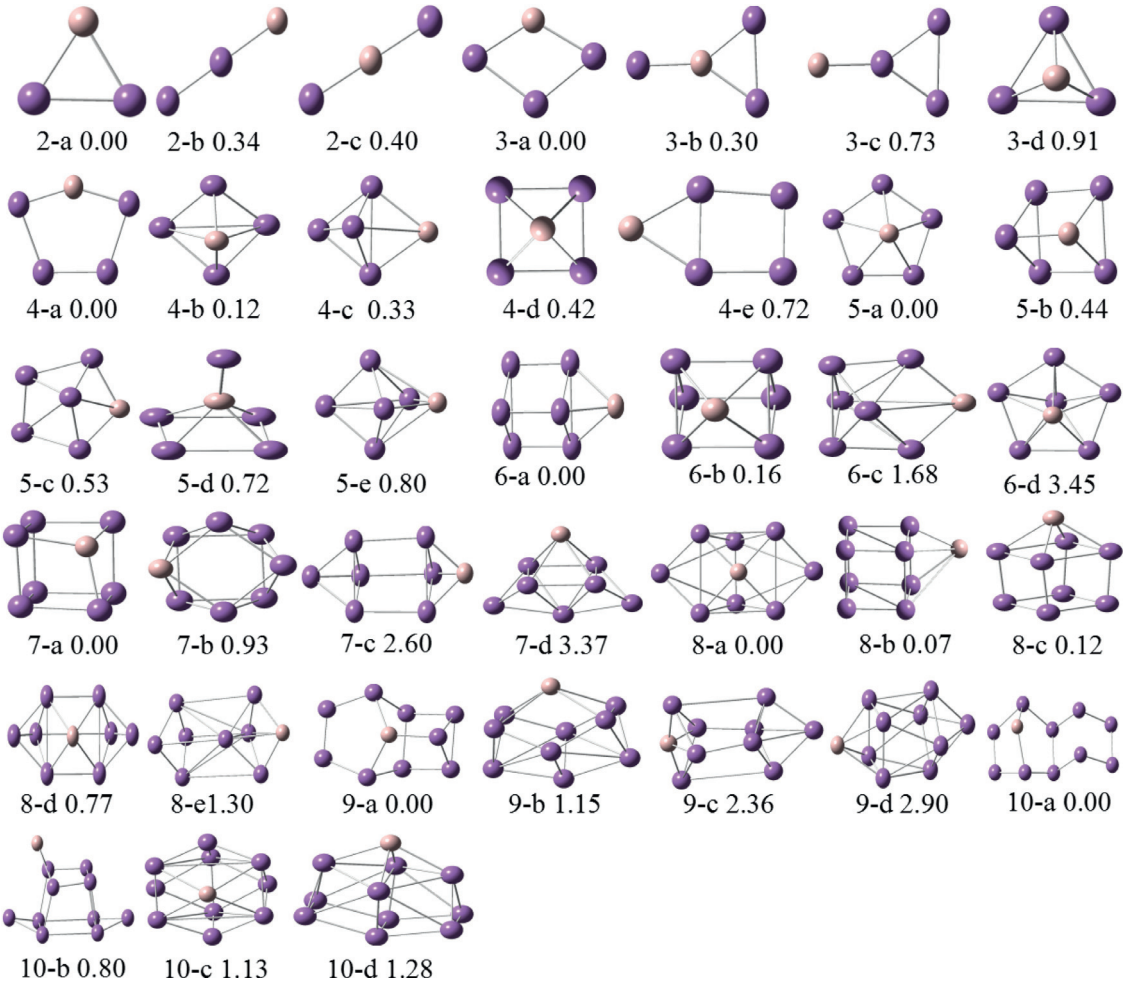

Fig. 1. The isomers structures of Sb_nAl clusters with n = 1–10.

B3P86/SDD, ω_e = 277.9 cm^{-1} for B3PW91/SDD) are very different from the experimental values (R_e = 2.342 Å [16], ω_e = 270.0 cm^{-1} [16]). As for Al_2, the B3P86/SDD and B3PW91/SDD results for the bond length (R_e = 2.561 Å for B3P86/SDD, R_e = 2.569 Å for B3PW91/SDD) is far from the experimental values (R_e = 2.7 Å [38]). From the Table 1, for Sb_2, the B3LYP/ LanL2DZ level yield R_e = 2.552 Å, ω_e = 263.3 cm^{-1}, and IP = 9.26 eV, for Al_2, the B3LYP/ LanL2DZ level yield R_e = 2.855 Å, ω_e = 235.1 cm^{-1}, and IP = 5.87 eV, which are more consistent with the experimental value, correspondingly. And the discussion suggests that the B3LYP/ LanL2DZ level is in excellent agreement with experimental results and other theory values.

During the process of choosing initial structures of the Sb_nAl clusters, we also considered the possible of isomeric structures. Then, based some independent configurations, we optimized several isomeric structures by placing an Al atom on each possible site of the Sb_n cluster or by adding one Sb atom to the $Sb_{n-1}Al$ cluster as well as by substituting one Sb by Al atom form the Sb_{n+1} cluster, we obtained the lowest energy structures of Sb_nAl clusters. We also implemented configurations calculations to gain ground state structures of $Sb_nAl^{\pm 1}$ (n = 1–10) clusters. In order to accurately obtain the most stable geometries of $Sb_{n-1}Al$ clusters, the possible spin multiplicities were also considered for overall isomers. For each isomer, the spin electronic configuration is considered at least from spins S = 1, 3, and 5, when n is an odd number. And the spin electronic configuration is considered at least from spins S = 2, 4, and 6, when n is even. All these calculations were carried out with the Gaussian 03 W package [40].

3. Results and discussion

3.1. Structures properties

The above approaches in part two have been found to be proven powerful and identified the ground states of nanoclusters. In this section, we would research the lowest energy structures of Sb_nAl (n = 1–10) and its low-lying isomers of Sb_nAl (n = 1–10). And we

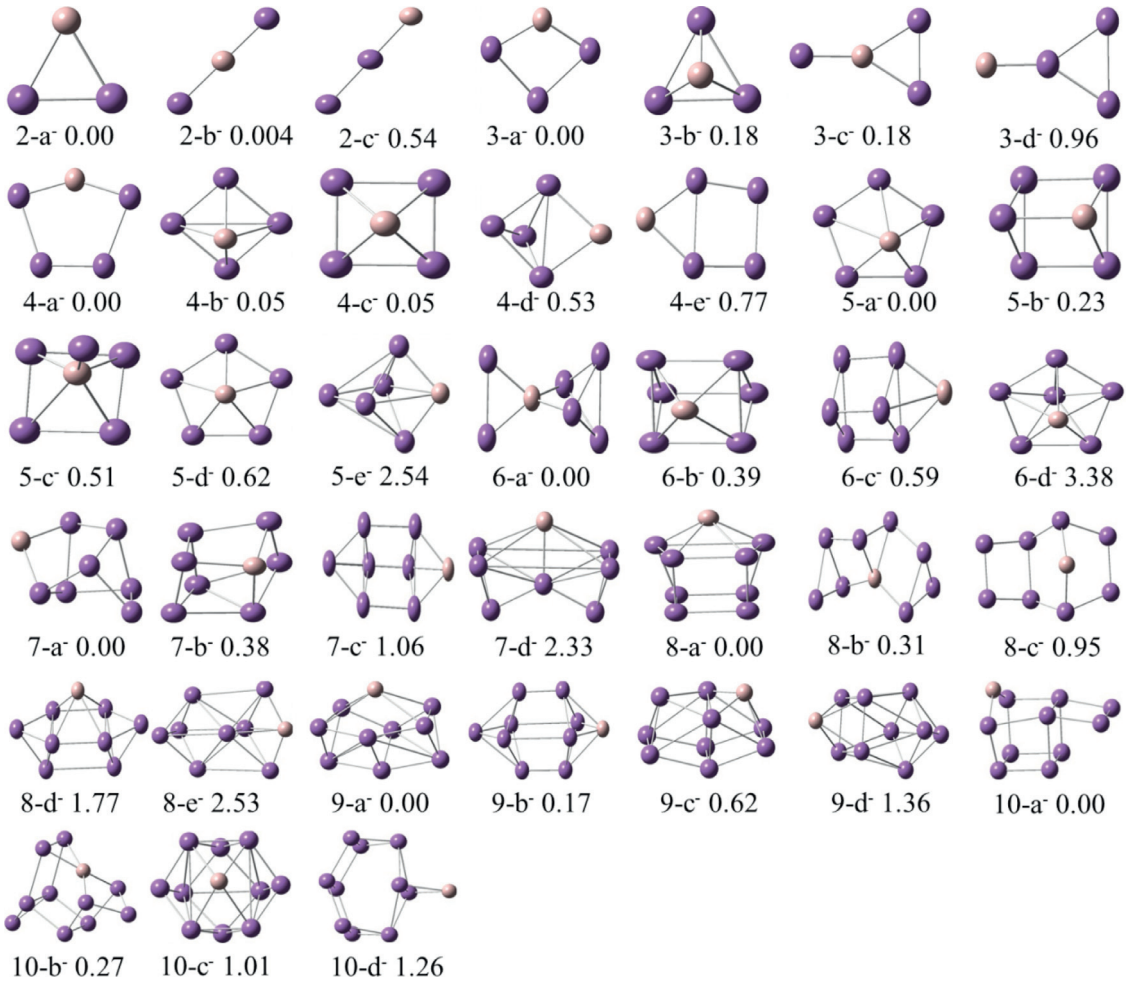

Fig. 2. The isomers structures of Sb_nAl^- clusters with n = 1–10.

used the computation scheme described in Sec. II to calculate these structures. The geometry structures of Sb_nAl (n = 1–10) and its isomers were depicted in Fig. 1. ((1) For these strings below the each model, the first one (number) represents the number of Sb atoms in the cluster, and the other ranks the isomer in the descending order of the binding energy. (2) In the picture, the atom Sb is shown as a purple sphere, and the other ball of color is Al. (3) The isomers are labeled as a, b, c, d and e in increasing order of their total energies or, equivalently, decreasing order of their relative stabilities). To compute the electron affinities of Sb_nAl (n = 1–10) clusters, we have also investigated the anionic Sb_nAl^- clusters and cationic Sb_nAl^+ up to n = 10. The lowest energy structures obtained for Sb_nAl^- and Sb_nAl^+ are shown in Fig. 2 and 3, respectively. For these structures, we calculated its spin multiplicities (S), point group symmetries (PG), the average bond length of Sb-Al bond (R_1), the average bond length Sb-Sb bond (R_2), and the corresponding electronic state (Sta), which are listed in Table 2. We had performed an extensive search to find the minimum energy structure in the way. In the case, for each n value, we first established some higher symmetry clusters model, and then we used the software of Gaussian to optimize and calculate each model. Finally, we selected some representative and lower energy clusters (shown in the Fig. 1, Fig. 2 and Fig. 3).

3.1.1. SbAl, $SbAl^-$ and $SbAl^+$

As for the $SbAl^{(0,\pm1)}$ clusters, they possess $C_{\infty V}$ symmetry. For the SbAl dimmer, the average bond length of Sb-Al (R_1) is 2.618 Å, the bond energy is 0.68 eV. The electronic state of $SbAl^-$ is $^2\Sigma$, the bond energy and the average bond length for $SbAl^-$ are 1.34 eV and 2.496 Å, respectively. In regard to $SbAl^+$ dimmer with $^4\Sigma$ electronic state, the 3.042 Å in average bond length and 0.33 eV in bond energy belong to them. Obviously, on the one hand, the bond energy of $SbAl^+$ cluster is the lowest among the $SbAl^{(0,\pm1)}$ clusters . On the other hand, the bond length of $SbAl^+$ is longer than the bond length of SbAl and $SbAl^-$. As far as the bond length and the bond energy are concerned, the Sb-Al interaction of the neutral SbAl is weaker than the Sb-Al interaction of the anionic $SbAl^-$.

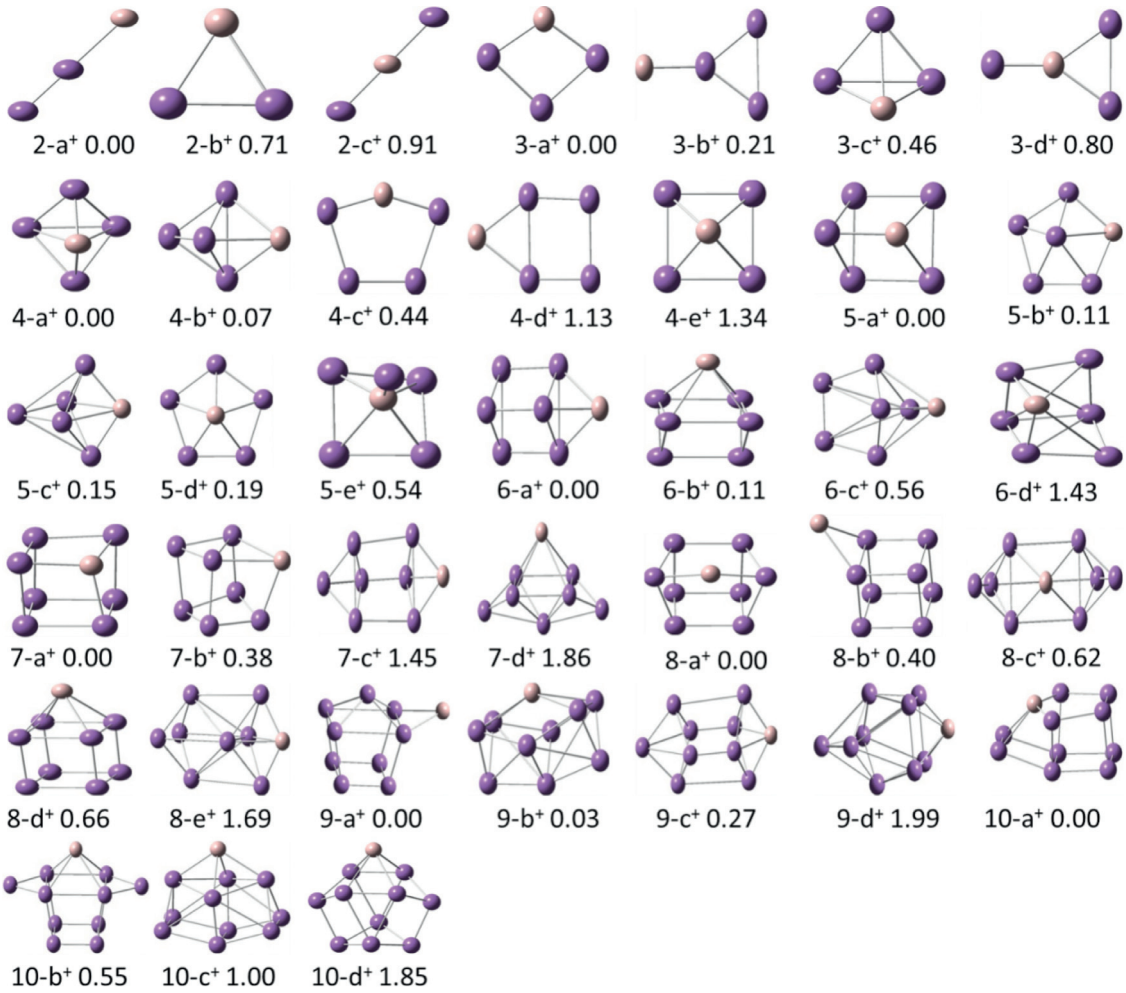

Fig. 3. The isomers structures of Sb_nAl^+ clusters with n = 1–10.

3.1.2. Sb_2Al, Sb_2Al^- and Sb_2Al^+

With regard to $Sb_2Al^{(0,\pm1)}$, that an aluminum atom interacts with two antimony atoms can form three structures including two line structures and a triangle structure. According to our calculation and optimization, the point group symmetry of the triangle structure is C_{2V}, the point group symmetries of line structures are $D_{\infty H}$ (the Al atom between the Sb atom and the Sb atom) and $C_{\infty V}$ (the Al atom at one end). As shown in the Fig. 1, Fig. 2 and Fig. 3, it is worth noting that the triangle structure is the lowest-energy structures for Sb_2Al cluster and Sb_2Al^- cluster. Nevertheless, the line structure of the Al atom at one end is the ground state structure for Sb_2Al^+. About triangle structure Sb_2Al cluster, the Al-Sb average bond length with 2.705 Å corresponding electronic state is $^2A_1$, the Sb-Sb bond length is 2.853 Å. Towards Sb_2Al^- clusters, the ground state structure with $^1A_1$ electronic state is named 2-a^- in Fig. 2, the Sb-Sb bond length and the Al-Sb average bond length of which are 2.761 Å, 2.936 Å, respectively. As the lowest-energy structure, the line structure (2-a^+) of the Al atom at one end has $^1\Sigma$ electronic state and 3.139 Å of Al-Sb bond length (R_1) and 2.541 Å of Sb-Sb bond length (R_2). According to the laws of physics, the reasons for that the R_1 or the R_2 is bigger or smaller than any other one being able to see easily in Table 2 is that the Al atom lose an electron, and the Al-Sb interaction becomes weaker and the Sb-Sb interaction becomes stronger. And the metastable structure named 2-b^+ in Fig. 3 owns $^3B_2$ of electronic state, 0.71 eV of binding energy to 2-a^+, 2.909 Å of Al-Sb bond length and 2.760 Å of Sb-Sb bond length.

3.1.3. Sb_3Al, Sb_3Al^- and Sb_3Al^+

In the case of $Sb_3Al^{(0,\pm1)}$, the ground-state structures and some low-lying isomers are optimized and listed in Fig. 1, Fig. 2 and Fig. 3, and the calculation results about $Sb_3Al^{(0,\pm1)}$ are listed in Table 2. From literature [22], we can guess that the tetragonal structure is the most stable for $Sb_3Al^{(0,\pm1)}$ clusters. Through these models and calculations, we can see that the neutral, anionic and cationic are possessed with the same most stable structure that is a planar quadrilateral structure, marked as 3-a, 3-a^- and 3-a^+, respectively. And those stable structures have the same symmetry which are C_{2v}. The other three geometries are a three-dimensional

Table 2
The spin multiplicities (S), point group symmetries (PG), the group state (Sta), and the average bond lengths of Sb–Al bond and Sb–Sb bond (R_1 and R_2) are listed.

	Neutral						Anionic							Cationic					
Clu.	Iso	PG	S	Sta	R_1	R_2	Clu.	Iso.	PG.	S	Sta	R_1	R_2	Clu.	Iso.	PG.	S	Sta	R_1	R_2
SbAl	1-a	$C_{\infty V}$	3	–	2.618	–	$SbAl^-$	1-a^-	$C_{\infty V}$	2	$^2\Sigma$	2.496	–	$SbAl^+$	1-a^+	$C_{\infty V}$	4	$^4\Sigma$	3.042	–
Sb_2Al	2-a	C_{2V}	2	$^2A_1$	2.705	2.853	Sb_2Al^-	2-a^-	C_{2V}	1	$^1A_1$	2.936	2.761	Sb_2Al^+	2-a^+	$C_{\infty V}$	1	$^1\Sigma$	3.139	2.541
	2-b	$C_{\infty V}$	2	–	2.776	2.627		2-b^-	$D_{\infty H}$	3	$^3\Sigma_G$	2.535	–		2-b^+	C_{2V}	3	$^3B_2$	2.909	2.760
	2-c	$D_{\infty H}$	4	–	2.601	–		2-c^-	$C_{\infty V}$	3	$^3\Sigma$	2.622	2.723		2-c^+	$D_{\infty H}$	5	$^5\Sigma_G$	2.735	–
Sb_3Al	3-a	C_{2V}	1	$^1A_1$	2.667	2.861	Sb_3Al^-	3-a^-	C_{2V}	2	$^2B_1$	2.596	3.009	Sb_3Al^+	3-a^+	C_{2V}	2	$^2A_2$	2.830	2.909
	3-b	C_{2V}	3	$^3A_2$	2.666	2.817		3-b^-	C_{3v}	2	$^2A_1$	2.797	3.056		3-b^+	C_{2V}	2	$^2B_1$	3.006	2.866
	3-c	C_{2V}	3	$^3B_2$	2.770	2.903		3-c^-	C_{2V}	2	$^2B_2$	2.686	2.786		3-c^+	C_{3v}	2	$^2A'$	2.740	2.871
	3-d	C_{3v}	1	$^1A_1$	2.664	3.194		3-d^-	C_{2V}	2	$^2A_2$	2.643	2.927		3-d^+	C_{2V}	2	$^2B_1$	2.690	2.734
Sb_4Al	4-a	C_S	2	$^2A''$	2.632	2.846	Sb_4Al^-	4-a^-	C_S	1	$^1A'$	2.590	2.853	Sb_4Al^+	4-a^+	C_{2V}	1	$^1A_1$	2.681	3.041
	4-b	C_{2V}	2	$^2B_2$	2.820	3.086		4-b^-	C_{2V}	1	$^1A_1$	–	2.887		4-b^+	C_S	1	$^1A_1$	–	3.007
	4-c	C_{4V}	2	$^2A_1$	3.121	2.978		4-c^-	C_{4V}	1	^1A	–	2.887		4-c^+	C_S	1	$^1A_1$	2.707	2.871
	4-d	C_S	2	$^2A''$	2.955	2.939		4-d^-	C_S	1	$^1A'$	3.036	3.008		4-d^+	C_S	1	$^1A'$	2.991	2.935
	4-e	C_S	2	$^2A''$	2.844	2.918		4-e^-	C_S	1	$^1A'$	2.790	2.917		4-e^+	C_{4V}	1	$^1A'$	2.781	3.040
Sb_5Al	5-a	C_{5V}	1	$^1A_1$	–	2.810	Sb_5Al^-	5-a^-	C_{5V}	2	^2A	3.108	2.850	Sb_5Al^+	5-a^+	C_S	2	$^2A''$	2.766	3.060
	5-b	C_S	1	1-A'	2.720	3.067		5-b^-	C_S	2	$^2A'$	2.909	3.014		5-b^+	C_S	2	$^2A'$	3.193	3.038
	5-c	C_S	1	1A'	2.964	3.032		5-c^-	C1	2	^2A	2.785	2.984		5-c^+	C_S	2	$^2A'$	2.841	3.053
	5-d	C_S	3	^3A	2.787	3.005		5-d^-	C_S	2	$^2A''$	2.956	2.971		5-d^+	C_{5V}	2	^2A	3.104	2.864
	5-e	C1	3	^3A	2.868	2.931		5-e^-	C_S	2	$^1A'$	3.070	3.011		5-e^+	C1	2	^2A	2.922	2.966
Sb_6Al	6-a	C_1	2	^2A	3.128	3.042	Sb_6Al^-	6-a^-	C_{2V}	1	$^1A_1$	2.767	2.959	Sb_6Al^+	6-a^+	C_1	1	^1A	3.074	3.052
	6-b	C_S	2	$^2A''$	–	3.074		6-b^-	C_S	1	$^1A'$	–	2.961		6-b^+	C_S	1	$^1A'$	–	3.055
	6-c	C_{2V}	4	$^4A_1$	3.003	2.962		6-c^-	C_1	1	^1A	3.033	3.070		6-c^+	C_{2V}	3	$^3B_1$	2.919	2.962
	6-d	C_{5V}	2	$^2A_1$	3.219	3.172		6-d^-	C_{5V}	1	$^1A_1$	–	3.140		6-d^+	C_S	5	$^1A_1$	2.850	3.025
Sb_7Al	7-a	C_S	3	$^1A'$	3.002	3.054	Sb_7Al^-	7-a^-	C_{3V}	2	$^2A_1$	2.763	3.057	Sb_7Al^+	7-a^+	C_1	2	^2A	2.703	3.014
	7-b	C_{3V}	1	$^1A_1$	2.687	3.054		7-b^-	C_1	2	^2A	2.803	2.989		7-b^+	C_S	2	$^2A'$	2.752	3.052
	7-c	C_1	1	^3A	2.740	3.014		7-c^-	C_S	2	$^2A'$	2.843	3.102		7-c^+	C_{3V}	2	^2A	–	3.022
	7-d	C_1	1	^1A	2.739	3.052		7-d^-	C_1	2	^2A	2.989	2.986		7-d^+	C_1	2	^2A	2.758	3.047
	7-e	C_{2V}	1	$^1A_1$	–	3.143		7-e^-	C_{2V}	4	$^4A_1$	2.857	2.959		7-e^+	C_{2V}	4	$^4B_1$	–	3.043
Sb_8Al	8-a	C_2	2	^2B	2.905	2.967	Sb_8Al^-	8-a^-	C_1	1	^1A	2.778	3.019	Sb_8Al^+	8-a^+	C_2	1	^1A	2.690	3.058
	8-b	C_S	2	$^2A'$	3.028	3.051		8-b^-	C_2	3	^3B	2.793	2.982		8-b^+	C_S	1	$^1A'$	3.142	3.054
	8-c	C_1	2	$^2A'$	–	3.028		8-c^-	C_S	3	$^3A''$	2.777	2.914		8-c^+	C_S	1	$^1A'$	–	2.989
	8-d	C_S	2	^2A	3.032	3.023		8-d^-	C_S	1	$^1A'$	3.205	2.992		8-d^+	C_1	3	^3A	2.813	3.019
	8-e	C_{2V}	4	$^4A_2$	2.835	2.948		8-e^-	C_{2V}	1	$^1A_1$	2.609	3.119		8-e^+	C_{2V}	3	$^3B_1$	2.660	3.023
Sb_9Al	9-a	C_S	1	$^1A'$	2.736	2.969	Sb_9Al^-	9-a^-	C_S	2	$^2A'$	3.011	3.066	Sb_9Al^+	9-a^+	C_S	2	$^2A''$	–	3.038
	9-b	C_S	1	$^1A'$	–	3.042		9-b^-	C_2	2	^2A	2.872	3.006		9-b^+	C_S	2	$^2A'$	–	3.071
	9-c	C_4	3	^3A	2.752	2.991		9-c^-	C_S	2	$^2A'$	2.926	3.071		9-c^+	C_2	2	2-B	2.699	3.046
	9-d	C_{4V}	1	$^1A_1$	–	3.023		9-d^-	C_{4V}	2	$^2B_2$	–	3.012		9-d^+	C_{4V}	4	$^4B_1$	2.995	3.132
$Sb_{10}Al$	10-a	C_S	2	$^2A'$	3.120	2.938	$Sb_{10}Al^-$	10-a^-	C_S	3	$^3A''$	2.690	3.063	$Sb_{10}Al^+$	10-a^+	C_S	1	$^1A'$	2.939	3.057
	10-b	C_S	4	$^4A''$	3.006	2.984		10-b^-	C_S	3	$^3A''$	2.843	2.959		10-b^+	C_S	3	$^3A'$	–	3.017
	10-c	C_{2V}	2	$^2A_1$	–	3.089		10-c^-	C_{2V}	1	$^1A_1$	–	3.078		10-c^+	C_{2V}	1	$^1A_1$	3.149	3.131
	10-d	C_{2V}	2	$^2B_1$	3.073	3.032		10-d^-	C_{2V}	1	$^1A_1$	3.048	3.078		10-d^+	C_{2V}	1	$^1A_1$	–	2.987

tetrahedral structure with C_{3v} symmetry, a planar Y-shaped structure with C_{2v} symmetry (An aluminum atom in the middle of the Y-shaped structure) and another planar Y-shaped structure with C_{2v} symmetry (An aluminum atom at the end of the Y-shaped structure), severally. The difference between 3-a (R_1 = 2.667 Å, R_2 = 2.861 Å), 3-a^- (R_1 = 2.596 Å, R_2 = 3.009 Å) and 3-a^+ (R_1 = 2.830 Å, R_2 = 2.909 Å) are the corresponding electronic state, which are $^1A_1$ of 3-a, $^2B_1$ of 3-a^-, $^2A_2$ of 3-a^+.

3.1.4. Sb_4Al, Sb_4Al^- and Sb_4Al^+

In terms of $Sb_4Al^{(0,\pm 1)}$ clusters, the lowest energy structure(4-a) for neutral Sb_4Al clusters is similar to the minimum energy structure(4-a^-) of Sb_4Al^- clusters, which is a plane pentagonal structure with C_S symmetry. Unlike 4-a and 4-a^-, the ground-state of cationic clusters is a hexahedron with C_{2V} symmetry. From the following figure, we can clearly see that the structure of 4-b is like the structure of 4-b^-, the structure of 4-d is similar to the structure of 4-c^-, the relative energy between 4-a the ground-state structure for Sb_4Al cluster and 4-b having a hexahedral structure is 0.12 eV, the relative energy of 4-d with quadrangular pyramid structure is 0.42 eV higher than 4-a. This shows that 4-b and 4-d are two completely different structures. But when 4-b gets an electron into 4-b^-, 4-d gets an electron into 4-c^-, 4-b^- and 4-c^- have almost the same relative energy (0.05 eV) to the ground state (4-a^-), In short 4-b^- and 4-c^- are almost the same structure. In cationic clusters, the ground state (4-a^+) is similar to 4-b, the cluster with quadrangular pyramid structure as 4-d is 4-e^+, the relative energy between 4-e^+ and 4-a^+(1.34 eV) is greater than the relative energy between 4-d and 4-b (0.3 eV).

3.1.5. Sb_5Al, Sb_5Al^- and $Sb5Al^+$

In so far as the $Sb_5Al^{(0,\pm1)}$ clusters are concerned, the lowest energy structures for neutral and anionic forms are similar and have the same symmetry (C_{5V}), but the most stable structure of cationic cluster with C_S symmetry is different with neutral and anionic forms. The pentagonal pyramid structure as the most stable structure for Sb_5Al neutral clusters has $^1A_1$ electronic state and 2.810 Å Sb-Sb bond length. Although the minimum energy structure for Sb_5Al^-clusters is similar to Sb_5Al clusters', their bond length (R_1 and R_2) and corresponding electronic state (Sta) aren't identical. The R_1, R_2 and Sta of $Sb_5Al^-$are 3.108 Å, 2.850 Å and ^{2}A, respectively. The most favorable geometry structure for Sb_5Al^+ clusters is a triangular prism structure possessed with R_1 = 2.766 Å, R_2 = 3.060 Å and ^{2}A" electronic state.

3.1.6. Sb_6Al, Sb_6Al^- and Sb_6Al^+

In the matter of $Sb_6Al^{(0,\pm1)}$, the most stable structure of Sb_6Al cluster (6-a) is formed by using one Sb atom to replace the Al atom of the structure named 5-b and then capping one Al atom on the triangular face of triangular prism structure of Sb_5Al cluster. We have also established and optimized several isomers, which are 6-b, 6-c, and 6-d. The relative energies of 6-b, 6-c and 6-d are 0.16 eV, 1.64 eV and 3.45 eV, respectively. The relative energies of 6-b^-, 6-c^- and 6-d^- are 0.39 eV, 0.59 eV and 3.38 eV respectively higher than the ground state (6-a^-). The bond energies of 6-b^+, 6-c^+ and 6-d^+ are 0.11 eV, 0.56 eV and 1.43 eV, respectively. It is obvious that the energy change range of anionic clusters and neutral clusters are larger than that of cationic clusters.

3.1.7. Sb_7Al, Sb_7Al^- and Sb_7Al^+

Considering the $Sb_7Al^{(0,\pm1)}$ clusters have eight atoms, our calculation and optimization to models confirm our guess that the cube structure is the minimum energy structure for the $Sb_7Al^{(0,\pm1)}$ clusters. But, the lowest energy structure for Sb_7Al^- cluster has a small change, because Sb_7Al^- has extra electronics, the interaction of aluminum atom with antimony atoms becomes more intense, and the cube structure becomes abnormal. Surely, this phenomenon is also suitable for all other anionic clusters. The most stable structure for Sb_7Al cluster is listed in Fig. 1 with ^{1}A' electronic state and C_S symmetry. The Al-Sb and Sb-Sb average bond lengths of 7-a are 2.739 Å and 3.054 Å, respectively. In terms of the ground state structure of Sb_7Al^- clusters (7-a^-), it has C_{3V} symmetry, $^2A_1$ electronic state, 2.763 Å in Al-Sb average bond length and 3.057 Å in Sb-Sb average bond length. Compared with 7-a and 7-a^-, the ground-state structure for Sb_7Al^+ clusters (7-a^+) has a lower symmetry which is C_1. Corresponding Al-Sb average bond length, Sb-Sb average bond length, and electronic state are 2.705 Å, 3.014 Å, and ^{2}A.

3.1.8. Sb_8Al, Sb_8Al^- and Sb_8Al^+

As far as the $Sb_8Al^{(0,\pm1)}$ clusters are concerned, we obtain five isomers, in which the spin doublet state is the spin state for the Sb_8Al clusters, in addition to the fifth structure, for which the spin state is the spin quartet state. By calculations, as to Sb_8Al^- clusters, the spin triplet state is the spin state of 8-a^- and 8-b^-. However, when we consider 8-c^-, 8-d^- and 8-e^-, the spin state is singlet. As shown in the Table 2, Sb_8Al^+ clusters have the spin singlet state (for 8-a^+, 8-b^+ and 8-c^+) and the spin triplet state (for 8-d^+ and 8-e^+). Even if they have the same spin state, but the electronic state is not the same. For example, the corresponding electronic state for 8-d^+ is ^{3}A, nevertheless, 8-e^+ is $^3B_1$.

3.1.9. Sb_9Al, Sb_9Al^- and Sb_9Al^+

For $Sb_9Al^{(0,\pm1)}$ clusters, after calculating, optimizing and selecting these model several times, we finally retained four isomers and listed them in Fig. 1, Fig. 2 and Fig. 3. With the increase in the number of atoms, the interaction between each atom is also enhanced. The binding energies are 1.71 eV, 1.79 eV, 1.54 eV for 9-a, 9-a^-, and 9-a^+. These ground state structures of $Sb_9Al^{(0,\pm1)}$ clusters are different from each other. And the lowest energy structure for Sb_9Al clusters with C_S symmetry and ^{1}A' electronic state is completely different from the minimum energy structure for Sb_9Al^- cluster with C_S symmetry and ^{2}A' electronic state. The most stable structure for Sb_9Al^+ cluster with C_S symmetry and ^{2}A" electronic state is not the same as the former two.

3.1.10. $Sb_{10}Al$, $Sb_{10}Al^-$ and $Sb_{10}Al^+$

In consideration of $Sb_{10}Al^{(0,\pm1)}$ clusters, the structure named 10-a in Fig. 1 is the ground-state structure of $Sb_{10}Al$ cluster. To our surprise, there is a great difference of structures between the isomers of $Sb_{10}Al$, $Sb_{10}Al^-$and $Sb_{10}Al^+$, in short, there is almost no similar structure. Our explanation is that not only the structures of clusters are charged, but also that each atom is subjected to multi-directional forces due to the larger number of atoms. In addition to the structures of this series of clusters, let us look at their characteristic parameters. The relative energy of 10-b is 0.8 eV higher than 10-a. However, the relative energy between 10-a^- and 10-b^- is only 0.27 eV. The ground state is marked 10-a^-, which has C_S symmetry, corresponding to electronic state, R_1 and R_2 are ^{3}A", 2.690 Å, and 3.063 Å, respectively. The most stable structure of $Sb_{10}Al^+$ cluster possesses C_s symmetry.

3.2. Relative stability

In order to study the stabilities of the most stable structures in each group of isomers, we calculated the averaged binding energy (E_b), fragmentation energy (E_f) and the second-order energy difference (Δ_2E) for each ground state structure. We referred to the averaged binding energies of Sb_n clusters in Document [23] so as to find the influence of Al atom doped antimony clusters. When we were doing these calculations, we did not think about entropy term, because that, in the density functional theory, the temperature is estimated at 0 k, and the entropy of the system will be zero at absolute zero, according to the third law of thermodynamics. The values of the oretical calculations of Sb_nAl, Sb_nAl^-, and Sb_nAl^+ (n = 1–10) clusters are defined in the following formula:

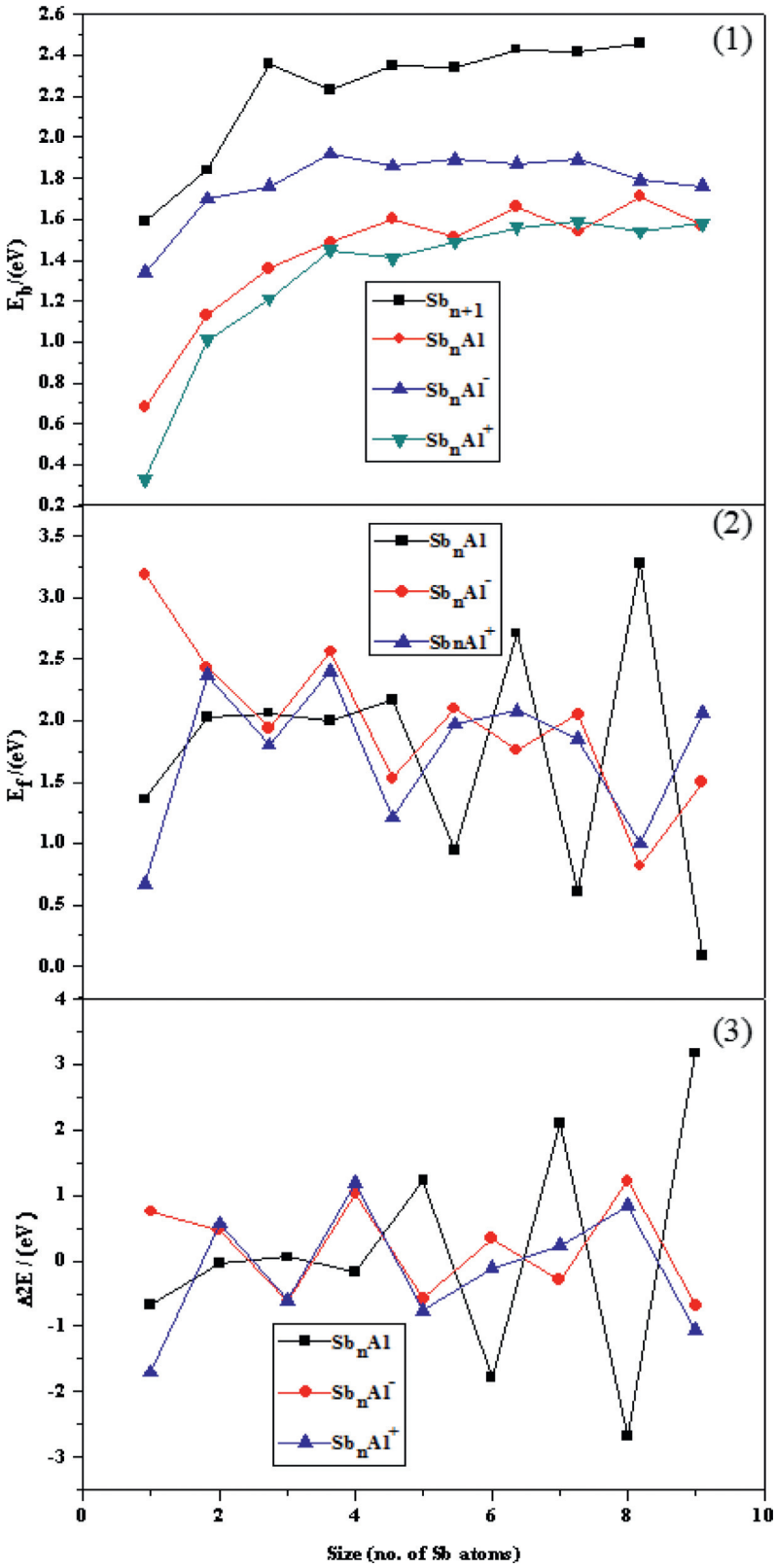

Fig. 4. Binding energies, fragmentation energies, and the second-order energy difference for the $Sb_nAl^{(0,\pm1)}$ (n = 1–10) clusters versus the number of antimony atoms.

$$E_b[Sb_nAl^{(0,\pm1)}] = (nE[Sb] + E[Al^{(0,+1)}] - E[Sb_nAl^{(0,\pm1)}])/(n+1), \quad (1)$$

$$E_b[Sb_nAl^{-}] = ((n-1)E[Sb] + E[Sb^{-}] + E[Al] - E[Sb_nAl^{-}])/(n+1), \quad (2)$$

$$E_f[Sb_nAl^{(0,\pm1)}] = E[Sb_{n-1}Al^{(0,\pm1)}] + E[Sb] - E[Sb_nAl^{(0,\pm1)}], \quad (3)$$

$$\Delta_2E[Sb_nAl^{(0,\pm1)}] = E[Sb_{n+1}Al^{(0,\pm1)}] + E[Sb_{n-1}Al^{(0,\pm1)}] - 2E[Sb_nAl^{(0,\pm1)}], \quad (4)$$

here, E is the total energy of relevant system. The values of E_b, E_f and Δ_2E for each Sb_nAl, Sb_nAl^-, and Sb_nAl^+ clusters are shown in Figs. 4(1), 4(2) and 4(3), respectively.

First of all, we can easily see from the Fig. 4(1) that the binding energies of $Sb_nAl^{(0,\pm1)}$ clusters is less stable than Sb_{n+1} clusters. This phenomenon shows that the doping of Al atoms into the antimony clusters reduces the stability of the Sb_n clusters. However, the doping of Al atoms into other pure clusters does not always increase the stability of the clusters. For example, the Sc_n clusters can be more stabilized after doping Al in the host clusters in previous theoretical study [41]. Then, as seen from Fig. 4(1), as for the average binding energies of Sb_nAl clusters, when the value of n is between 4 and 10, the values of binding energy show slight oscillation. For the average binding energies of Sb_nAl^- clusters, they show an increasing trend when n is less than 4 and a decreasing trend when n is greater than 4, which means that the maximum is obtained when n is equal to 4. In general, anionic clusters have a higher averaged binding energy than neutral clusters, whose averaged binding energy is higher than those of cationic clusters.

The second, as shown in Fig. 4(2), both the charged clusters and the neutral clusters present oscillations in fragmentation energy. For neutral clusters, when n takes 3, 5 and 7, the values of fragmentation energy are at the peak of oscillation. For the Sb_nAl^- clusters, the fragmentation energies exhibit a pronounced odd-even oscillation behavior as a function of cluster size, except Sb_2Al^-. In terms of the fragmentation energies of Sb_nAl^+ clusters, when n takes 4, the fragmentation energy has the maximum value that is 2.40 eV. It means that Sb_4Al^+ cluster are more stable than other clusters.

The last, to further illustrate the relative stabilities of the clusters, we calculated the second-order difference energy of each ground state structure, are displayed in Fig. 4(3). When the values of Δ_2E are positive, the dissociation of Sb atom is unfavorable process and the clusters are particularly stable. Well, in the case of n taking 3, 5, 7 and 9, the values of Δ_2E are positive for neutral clusters. Under the situation of n taking 1, 2, 4, 6 and 8, the Δ_2Es of anionic clusters are positive. When n is equal to 2, 4, 7 and 8, in the case of cationic clusters, the values of Δ_2E are positive. In short, these structures are relatively stable. These cases also cater to the stability of the cluster through the binding energy.

3.3. Natural population analysis

We not only analyzed the structural stability in terms of energy, we also analyzed the electron transfer within each cluster. We calculated the amount of charge that each atom in the cluster by calculating the natural bond orbital (NBO) of $Sb_{1-10}Al$ and $Sb_{1-10}Al^{(\pm1)}$ clusters. The total natural charges of Al atoms and the total natural charges of Sb atoms are shown in Table 3. In neutral Sb_nAl clusters, the total charge on the Al atom has a positive value (or negative value) and the total charge on the Sb atom has a negative value (or positive value), which indicates that the charge shift in the cluster. Since there is a charge transfer between the Al atom and the Sb atom, and from Table 3 we can see that the charge transfer of Sb and Al atoms are less than an electron, it indicates that the covalent bond rather than the ionic bond is formed between the Sb atom and the Al atom in the cluster.

For Sb_nAl^-, the charges on the Sb and Al atoms of $Sb_{1\text{-}4,\ 8,\ 10}Al^-$ clusters have negative values. For $Sb_{5\text{-}7,\ 9}Al^-$ clusters, the Sb atoms have negative values but Al atoms have positive values, that is to say, the electron is transferred from Al atom to Sb frames. Sb_nAl^+ clusters are particularly attractive to us due to the negative charge value of Sb in Sb_2Al^+ cluster. This may be caused by its special structure. From this structure, three atoms are located in the same line, and there are two Sb atoms acting on the same side of the Al atom to give the Al atom a force, however, there is no force in other directions. As a result, Sb also exhibits a negative charge, even if the entire cluster is positively charged.

Table 3
The total charges (Q) of Sb atoms and the charges (Q) of Al atom for the ground state structures of $Sb_nAl^{(0,\pm1)}$ clusters.

	Q(Sb)	Q(Al)		Q(Sb)	Q(Al)		Q(Sb)	Q(Al)
SbAl	−0.218	0.218	$SbAl^-$	−0.672	−0.328	$SbAl^+$	0.215	0.785
Sb_2Al	−0.200	0.200	Sb_2Al^-	−0.966	−0.034	Sb_2Al^+	−0.035	1.035
Sb_3Al	−0.094	0.094	Sb_3Al^-	−0.946	−0.054	Sb_3Al^+	0.633	0.367
Sb_4Al	0.032	−0.032	Sb_4Al^-	−0.935	−0.065	Sb_4Al^+	0.686	0.314
Sb_5Al	−0.341	0.341	Sb_5Al^-	−1.172	0.172	Sb_5Al^+	0.710	0.290
Sb_6Al	−0.404	0.404	Sb_6Al^-	−1.542	0.542	Sb_6Al^+	0.333	0.667
Sb_7Al	−0.308	0.308	Sb_7Al^-	−1.137	0.137	Sb_7Al^+	0.731	0.269
Sb_8Al	0.029	−0.029	Sb_8Al^-	−0.857	−0.143	Sb_8Al^+	0.714	0.286
Sb_9Al	−0.277	0.277	Sb_9Al^-	−1.066	0.066	Sb_9Al^+	0.255	0.745
$Sb_{10}Al$	−0.187	0.187	$S_{b10}Al^-$	−0.860	−0.140	$Sb_{10}Al^+$	0.774	0.226

3.4. Electronic properties

In this section, our calculations contain the energy gap (E_g) between the highest occupied molecular orbital (HOMO) and the lowest unoccupied molecular orbital (LUMO), the electronic properties including adiabatic electron affinity (AEA), vertical electron detachment energy (VDE), adiabatic ionization potential energy (AIP), vertical ionization potential energy (VIP). We calculated values of the AEA, VDE, AIP, and VIP using the following method.

$$AEA = E(optimized\ neutral) - E(optimized\ anion), \tag{5}$$

$$VDE = E(neutral\ at\ optimized\ anion\ geometry) - E(optimized\ anion), \tag{6}$$

$$AIP = E(optimized\ cation) - E(optimized\ neutral), \tag{7}$$

$$VIP = E(cation\ at\ optimized\ neutral\ geometry) - E(optimized\ neutral), \tag{8}$$

$$E_g = E(\text{thelowest unoccupied molecular orbital}) - E(\text{the highest occupied molecular orbital}) \tag{9}$$

here, E is the total energies of the corresponding systems. The results of our calculations about AEA, VDE, AIP, VIP, and E_g are shown in Fig. 5 (5(1), 5(2), 5(3)). First, the larger value of HOMO-LUMO energy gap is, the poorer ability of a cluster to participate in chemical reaction is. From the Fig. 5 we can also see that the stabilities of clusters with odd n are higher than the stabilities of clusters with even n in neutral clusters, except Sb_3Al cluster. In anionic clusters, it's just the opposite, the stabilities of clusters with even n are higher the stabilities of clusters with odd n, except for Sb_2Al^- cluster. Three remarkable peaks at n = 1, 4, and 7 for Sb_nAl^+ clusters are found, which indicate that the $SbAl^+$, Sb_4Al^+, and Sb_7Al^+ clusters possess dramatically enhanced chemical stabilities.

From Fig. 5(2) and Fig. 5(3), Fig. 5(2) shows that the AEAs and VDEs have obvious odd-even alteration as the size n increases, and the alteration behaviors are coincident from n = 5–10. This phenomenon indicates that the ionizations of the Sb_6Al, Sb_8Al, and $Sb_{10}Al$ clusters are more hard ionized than the neighbor clusters. It is seen from Fig. 5(3) that the AIPs are always larger than the VIPs. The AIPs and VIPs have obvious odd-even alteration from n = 4–10, the alteration behaviors are contrary with AEAs and VDEs. We can also see that any value of AIP is greater than the value of AEA. This shows that the neutral cluster (Sb_nAl) is more likely to get electrons into a negatively charged cluster than to lose the electron into a positively charged cluster. This phenomenon occurs not only in our calculations, but also in other articles [24,42].

3.5. Magnetisms

We displayed the results of the magnetic moment of ground-state clusters in Fig. 6. We can also see that the total magnetic moments of the Sb_nAl clusters show an obvious odd-even alternative behavior, when n is an odd number, the magnetic moment of the neutral cluster is zero, except for SbAl cluster. What is very interesting is that the cation clusters have the same magnetic moment as the anion clusters, when n is between 2 and 9, which also show odd-even alternative behavior, but the alternative behaviors are contrary with the neutral Sb_nAl clusters. The $SbAl^{\pm 1}$, $Sb_3Al^{\pm 1}$, $Sb_5Al^{\pm 1}$, $Sb_7Al^{\pm 1}$, and $Sb_9Al^{\pm 1}$ clusters exhibit magnetic moments, but the most stable $Sb_2Al^{\pm 1}$, $Sb_4Al^{\pm 1}$, $Sb_6Al^{\pm 1}$, $Sb_8Al^{\pm 1}$, and $Sb_{10}Al^{-1}$ clusters exhibit nonmagnetic moments, that is to say, the $SbAl^{\pm 1}$, $Sb_3Al^{\pm 1}$, $Sb_5Al^{\pm 1}$, $Sb_7Al^{\pm 1}$, $Sb_9Al^{\pm 1}$, and $Sb_{10}Al^{+1}$ clusters magnetic structures, the other isomers are nonmagnetic structures.

4. Conclusions

The geometrical and electronic properties of small Al-doped Sb_n clusters (n = 1–10) are investigated with hybrid B3LYP functional. In this task, after our systematic study towards the $Sb_nAl^{(0,\pm 1)}$ clusters, we obtain the following conclusion:

The geometries show that there is a certain difference between the ground state structures of Sb_nAl, Sb_nAl^-, and Sb_nAl^+ clusters. When n is taken 3, the ground state of $Sb_3Al^{(0,\pm 1)}$ clusters have the same geometry structure. When n takes other values (1, 2, 4–10), the most stable structures of $Sb_nAl^{(0,\pm 1)}$ clusters are not the same. As the value of n increases, the bond energy roughly increases and then flattens. The fragmentation energy (E_f) and the second-order energy difference (Δ_2E) show the oscillation behavior. By analyzing the relative stabilities of $Sb_nAl^{(0,\pm 1)}$ clusters as n changes, we obtain this conclusion that the Sb_5Al, Sb_7Al, and Sb_9Al clusters are relatively stable for neutral clusters, Sb_2Al^-, Sb_4Al^-, and Sb_7Al^- clusters are relatively stable for anionic clusters, Sb_4Al^+, Sb_6Al^+, and Sb_8Al^+ clusters relatively stable for cationic clusters.

The natural population analysis of Sb_nAl clusters show that the charges transfer from Al atom to Sb frames, expect Sb_4Al and Sb_8Al clusters. However, the charges of Sb_nAl^- clusters on all the Sb and Al atoms have negative values, except for $Sb_{5\text{-}7,\ 9}Al$ clusters, and the charges of Sb_nAl^+ clusters on all the Sb and Al atoms have positive values, in addition to Sb_2Al^+. After analyzing the HOMO-LUMO gaps, AEA, VDE, AIP, and VIP, the variety of HOMO-LUMO gaps both Sb_nAl and Sb_nAl^- are opposite, except for n = 1, 3, and 10, the neutral Sb_nAl clusters are easier to get the electron than to lose the electron, and Sb_9Al clusters are not more easily ionized than the others. In aspect of magnetism, Sb_nAl^{-1} and Sb_nAl^{+1} clusters have the same trend of change, apart from $Sb_{10}Al^{\pm 1}$. Compared with $Sb_nAl^{\pm 1}$, the trend of change about magnetisms of Sb_nAl clusters happens to be the opposite, besides SbAl.

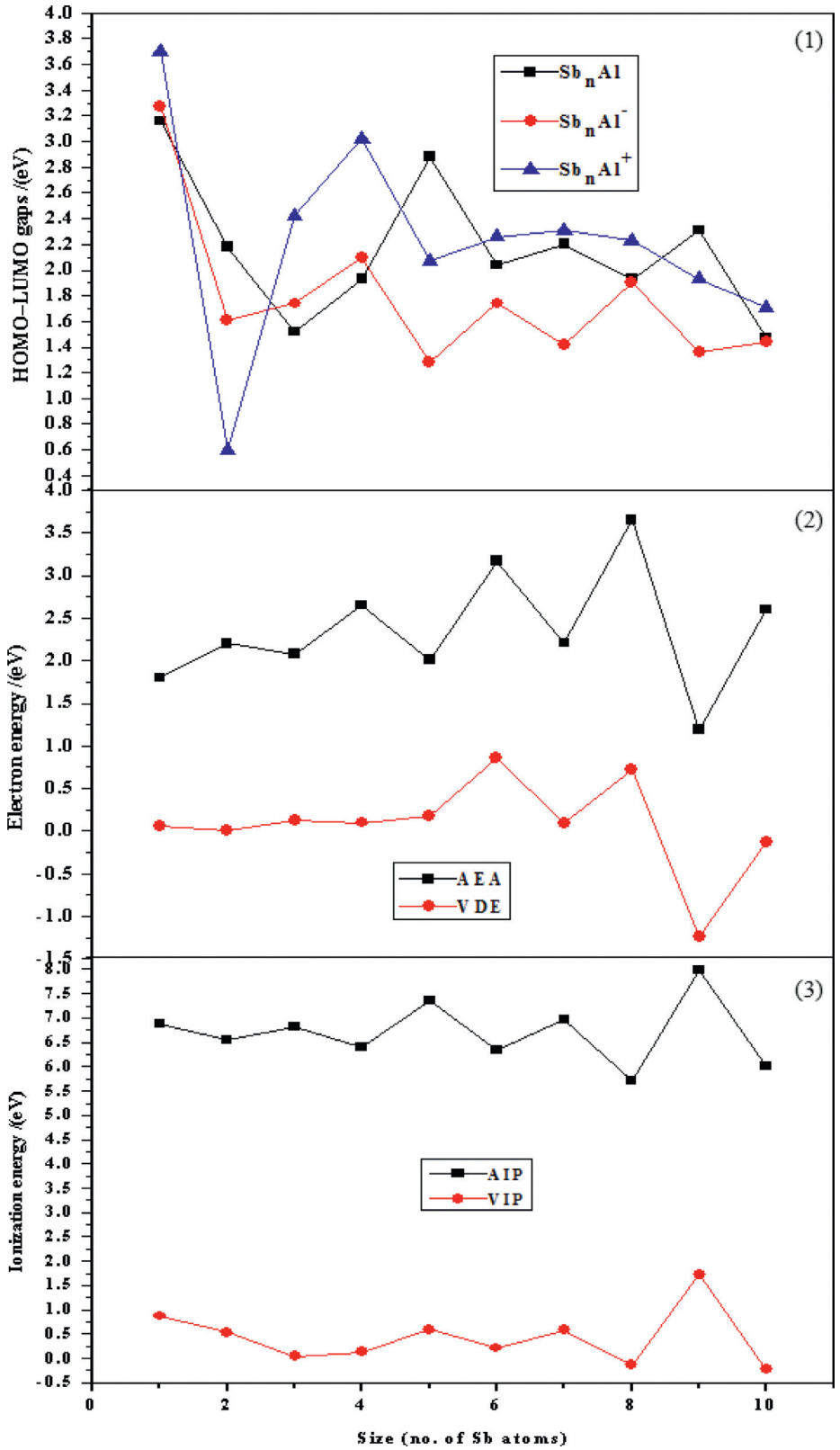

Fig. 5. HOMO–LUMO gaps, electron energies, and ionization energies for the $Sb_nAl^{(0,\pm 1)}$ (n = 1–10) clusters versus the number of Sb atoms.

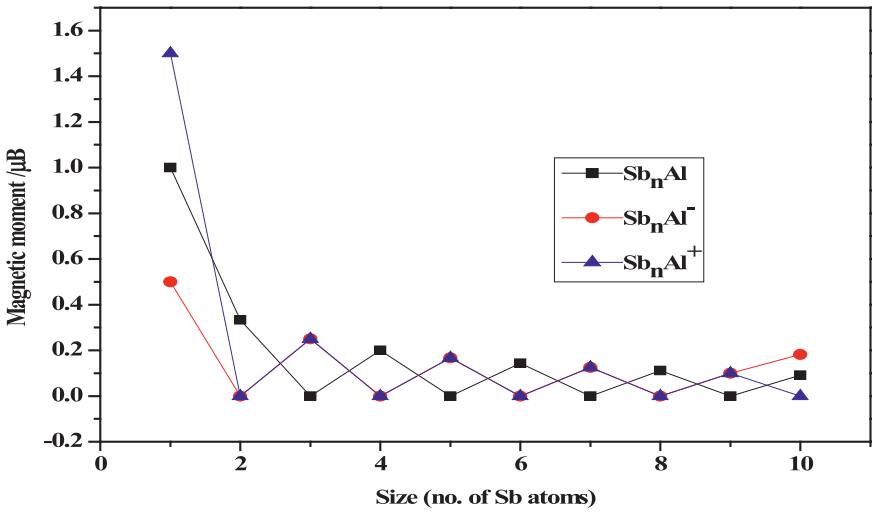

Fig. 6. Magnetic moment for the $Sb_nAl^{(0,\pm 1)}$ (n = 1–10) clusters versus the number of Sb atoms.

Acknowledgements

This research is supported by Cultivating Programme of Excellent Innovation team of Chengdu University of Technology (Grant No. JXTD20176) and Cultivating Programme of Middle-aged backbone teachers of Chengdu University of Technology (10912-KYGG201512). We acknowledge Project supported by the National Natural Science Foundation of China (No. 11404042), and the Science & Technology Department of Sichuan Province (No. 2016RZ0069). This work is also supported by the Research Foundation of Chengdu University of Technology (No. 2017YJ04) and Student's Platform for Innovation and Entrepreneurship Training Program (201710616143).

Supplementary materials

Supplementary material associated with this article can be found, in the online version, at doi:10.1016/j.cjph.2018.05.003.

References

[1] P. Jensen, Growth of nanostructures by cluster deposition: experiments and simple models, Rev. Mod. Phys 71 (1999) 1695–1735.
[2] R. Sessoli, D. Gatteschi, A. Caneschi, M.A. Novak, Magnetic bistability in a metal-ion cluster, Nature 365 (1993) 141–143.
[3] W. Huang, A.P. Sergeeva, H.J. Zhai, B.B. Averkiev, L.S. Wang, A.I. Boldyrev, A concentric planar doubly p-aromatic B192 cluster, Nat. Chem 2 (2010) 202–206.
[4] D. Chrobak, N. Tymiak, A. Beaber, O. Ugurlu, W.W. Gerberich, R. Nowak, Deconfinement leads to changes in the nanoscale plasticity of silicon, Nat. Nanotechnol. 6 (2011) 480–484.
[5] J.A. Alonso, Electronic and atomic structure, and magnetism of Transition-Metal clusters, Chem. Rev. 100 (2000) 637–678.
[6] R. Ferrando, J. Jellinek, R.L. Johnston, Nanoalloys: From theory to applications of alloy clusters and nanoparticles, Chem. Rev. 108 (2008) 845–910.
[7] H.Q. Wang, X.Y. Kuang, H.F. Li, Density functional study of structural and electronic properties of bimetallic copper–gold clusters: comparison with pure and doped gold clusters, Phys. Chem. Chem. Phys. 12 (2010) 5156–5165.
[8] J.G. Du, X.Y. Sun, G. Jiang, A DFT study on small M-doped titanium (M = V, Fe, Ni) clusters: structures, chemical bonds and magnetic properties, The European Physical Journal D. 55 (2009) 111–120.
[9] L.M. Prates, G.B. Ferreira, J.W.M. Carneiro, W.B. de Almeida, A.N.M. Carauta, J.C.G. Correiad, M.T.M. Cruz, The Effect of Gamma-Al2O3 Support on the NO Adsorption on Pd4 Cluster, J. Braz. Chem. Soc. 2 (2016) 2062–2069.
[10] S. Yin, R. Moro, X. Xu, W.A. de Heer, Magnetic enhancement in Cobalt-Manganese alloy clusters, Phys. Rev. Lett. 98 (2007) 113401-1-4.
[11] R.A. Guirado-Lopez, F. Aguilera-Granja, Bimetallic Fe-Ni cluster alloys: Stability of core(Fe)-shell(Ni) arrays and their role played in the structure and magnetic behavior, J.Phys. Chem. C 112 (2008) 6729–6739.
[12] (a)A.J. Hoffman, L. Alekseyev, S.S. Howard, K.J. Franz, D. Wasserman, V.A. Podolskiy, E.E. Narimanov, D.L. Sivco, C. Gmachl, Negative refraction in semiconductor metamaterials, Nat. Mater. 6 (2007) 946–950;
(b) E.V. Shevchenko, D.V. Talapin, S. O'Brien, C.B. Murray, Polymorphism in AB13 nanoparticle superlattices: An example of semiconductor-metal metamaterials, J. Am. Chem. Soc. 127 (2005) 8741–8747;
(c) I. Vurgaftman, J.R. Meyer, L.R. Ram-Mohan, Band parameters for III-V compound semiconductors and their alloys, J. Appl. Phys. 89 (2001) 5815–5875;
(d) L. Galfetti, L.T. De Luca, F. Severini, L. Meda, G. Marra, M. Marchetti, M. Regi, S. Bellucci, Nanoparticles for solid rocket propulsion, J. Phys.: Condens. Matter 18 (2006) S1991–S2005.
[13] K. Ikarashi, J. Sato, H. Kobayashi, S. Saito, H. Nishiyama, Y. Inoue, Photocatalysis for water decomposition by RuO2-dispersed ZnGa2O4 with d^{10} configuration, J. Phys. Chem. B 106 (2002) 9048–9053.
[14] J. Kordis, K.A. Gingerich, Mass spectroscopic investigation of the equilibrium dissociation of gaseous Sb_2, Sb_3, Sb_4, SbP, SbP_3, and P_2, J. Chem. Phys. 58 (1973) 5141–5149.
[15] G. Gerber, G. Kuscher, Laser induced fluqrescence of Sb2.I. v isible B-X system, Chem. Phys. 60 (1981) 119–131.
[16] K.P. Huber, G. Herzberg, Molecular spectra and molecular structure, IV. Constants of Diatomic Molecules, Van Nostrand Reinhold, New York, 1979.
[17] M.E. Geusic, R.R. Freeman, M.A. Duncan, Photofragmentation of antimony and bismuth cluster cations at 248nm, J. Chem. Phys. 88 (1988) 163–166.
[18] M.E. Geusic, R.R. Freeman, M.A. Duncan, Neutral and ionic clusters of antimony and bismuth: A comparison of magic numbers, J. Chem. Phys. 89 (1988)

223–229.
[19] L.S. Wang, Y.T. Lee, D.A. Shirley, Photoelectron spectroscopy and electronic structure of clusters of the group V elements. III. Tetramers: The 2T2 and 2At excited states of P_4^+, As_4^+ and Sb_4^+, J. Chem. Phys. 93 (1990) 1–21.
[20] M.L. Polak, G. Gerber, J. Ho, W.C. Lineberger, Photoelectron spectroscopy of small antimony cluster anions: Sb^-, $Sb2^-$, $Sb3^-$, and $Sb4^-$, J. Chem. Phys. 97 (1992) 8990–9000.
[21] M. Gausa, R. Kaschner, G. Seifert, J.H. Faehrmann, H.O. Lutz, K.-H. Meiwes-Broer, Photoelectron investigations and density functional calculations of anionic Sb_n- and Bi_n- clusters, J. Chem. Phys. 104 (1996) 9719–9728.
[22] F. Hagelberg, S. Neeser, N. Sahoo, T.P. Das, Geometry and bonding in alkali-metal-atom —antimony (A„Sb4) clusters, Phys. Rev. A. 50 (1994) 557–566.
[23] X.L. Zhou, J.J. Zhao, X.S. Chen, W. Lu, Structural and electronic properties of Sb_n (n = 2–10) clusters using density-functional theory, Phys. Rev. A 72 (2005) 053203-1-6.
[24] S.P. Shi, Y.L. Liu, B.L. Deng, C.Y. Zhang, G. Jiang, Geometries, stabilities, and electronic properties of small GanTi(0, ± 1) (n = 1–10) clusters studied by density functional theory, Comput, Mater. Sci. 95 (2014) 476–483.
[25] J.G. Du, X.Y. Sun, G. Jiang, Structures, chemical bonding, magnetisms of small Al-doped zirconium clusters, Phys. Lett. A 374 (2010) 854–860.
[26] C.J. Wu, P.F. Lu, Z.Y. Yu, L. Ding, Y.M. Liu, L.H. Han, Structural and electronic properties of neutral clusters $Al_{12}X$ (X = P, As, Sb, and Bi) and their cations, Comput. Theor. Nanosci. 10 (2013) 1055–1060.
[27] J.J. Melko, P.A. Clayborne, C.E. Jones, Jr., J.U. Reveles, U. Gupta, S.N. Khanna, A.W. Castleman, Jr., Combined experimental and theoretical study of Al_nX (n = 1-6; X = As, Sb) clusters: evidence of aromaticity and the jellium model, J. Phys. Chem. A. 114 (2010) 2045–2052.
[28] N.L. Hadipour, A.A. Peyghan, H. Soleymanabadi, Theoretical study on the Al-Doped ZnO nanoclusters for CO chemical sensors, J. Phys. Chem. C 119 (11) (2015) 6398–6404.
[29] L.X. Zhao, X.J. Feng, T.T. Cao, X. Liang, Y.H. Luo, Density functional study of Al-doped Au clusters, Chin. Phys. B 18 (2009) 2709–2718.
[30] J.T. Ziebarth, J.M. Woodall, R.A. Kramer, G. Choi, Liquid phase-enabled reaction of Al-Ga and Al-Ga-In-Sn alloys with water, Hydrogen Energy 36 (2011) 5271–5279.
[31] D.E. Bergeron, P.J. Roach, A.W. Castleman, Jr., N.O. Jones, S.N. Khanna, Al cluster superatoms as halogens in polyhalides and as alkaline earths in iodide salts, Science 307 (2005) 231–235;
[31a] J.U. Reveles, S.N. Khanna, P.J. Roach, A.W. Castleman, Jr., Multiple valence superatoms, Proc. Natl. Acad. Sci. U. S. A. 103 (2006) 18405–18410;
[31b] A.W. Castleman, Jr., S.N. Khanna, Clusters, superatoms, and building blocks of new materials, J. Phys. Chem. C 113 (2009) 2664–2675.
[32] A.D. Becke, Density-functional exchange-energy approximation with correct asymptotic behavior, Phys. Rev. A 38 (1988) 3098–3100.
[33] C. Lee, W. Yang, R.G. Parr, Development of the Colle-Salvetti correlation-energy formula into a functional of the electron density, Phys. Rev. B 27 (1988) 785–789.
[34] W.R. Wadt, P.J. Hay, Ab initio effective core potentials for molecular calculations. Potentials for main group elements Na to Bi, J. Chem. Phys. 82 (1985) 284–298.
[35] L.S. Wang, Y.T. Lee, D.A. Shirley, K. Balasubramanian, P. Feng, Photoelectron spectroscopy and electronic structure of clusters of the group V elements. I. dimers, Chem. Phys. 93 (1990) 1–24.
[36] Y.L. Liu, Y.W. Hua, M. Jiang, G. Jiang, J. Chen, Theoretical study of the geometries and dissociation energies of molecular water on neutral aluminum clusters Al_n (n = 2–25), Chem. Phys. 136 (2012) 084703-1-9.
[37] J. Akola, H. Häkkinen, M. Manninen, Ionization potential of aluminum clusters, Phys. Rev. B 58 (1998) 3601–3604.
[38] M.F. Cai, T.P. Dzugan, V.E. Bondybey, Fluorescence studies of laser vaporized aluminum: evidence for A 3Πμ, ground state of aluminum dimer chemical physics 115 (1989) 4–5.
[39] A.I. Boldyrev, J. Simons, Periodic table of diatomic molecules. Part A, Diatomics of Main Group Elements [M], Wiley, London, 1997.
[40] M.J. Frisch, G.W. Trucks, H.B. Schlegel, G.E. Scuseria, M.A. Robb, J.R. Cheeseman, J.A. Montgomery Jr, T. Vreven, K.N. Kudin, J.C. Burant, J.M. Millam, S.S. Iyengar, J. Tomasi, V. Barone, B. Mennucci, M. Cossi, G. Scalmani, N. Rega, G.A. Petersson, H. Nakatsuji, M. Hada, M. Ehara, K. Toyota, R. Fukuda, J. Hasegawa, M. Ishida, T. Nakajima, Y. Honda, O. Kitao, H. Nakai, M. Klene, X. Li, J.E. Knox, H.P. Hratchian, J.B. Cross, C. Adamo, J. Jaramillo, R. Gomperts, R.E. Stratmann, O. Yazyev, A.J. Austin, R. Cammi, C. Pomelli, J.W. Ochterski, P.Y. Ayala, K. Morokuma, G.A. Voth, P. Salvador, J.J. Dannenberg, V.G. Zakrzewski, S. Dapprich, A.D. Daniels, M.C. Strain, O. Farkas, D.K. Malick, A.D. Rabuck, K. Raghavachari, J.B. Foresman, J.V. Ortiz, Q. Cui, A.G. Baboul, S. Clifford, J. Cioslowski, B.B. Stefanov, G. Liu, A. Liashenko, P. Piskorz, I. Komaromi, R.L. Martin, D.J. Fox, T. Keith, M.A. Al-Laham, C.Y. Peng, A. Nanayakkara, M. Challacombe, P.M.W. Gill, B. Johnson, W. Chen, M.W. Wong, C. Gonzalez, J.A. Pople, Gaussian 03, Revision B 02, Gaussian, Inc, Pittsburgh PA, 2003.
[41] F.Y. Tian, Q. Jing, Y.X. Wang, Structure, stability, and magnetism of Sc_nAl (n = 1-8, 12) clusters: Density-functional theory investigations, Phys. Rev. A 77 (2008) 013202-1-8.
[42] S.P. Shi, C.Y. Zhang, X.F. Zhao, X. Li, M. Yan, G. Jiang, Geometries, stabilities, and electronic properties analysis in $In_nNi^{(0,\pm 1)}$ clusters: Molecular modeling and DFT calculations, Chin. Phys. B 26 (2017) 083103-1-10.